CHAPTER IV

RESULTS

4.1 Introduction

Meticulous analysis of receiver functions derived from stations of TOR and SVEKALAPKO networks (Fig. 4.1) have resulted in mapping of the Moho topography and valuable information on major intracrustal features, specially those associated with ancient suture zones in studied region. The upper mantle 410 km and 660 km discontinuities have also been the focus of this investigation and their behavior in known structural domains are profiled.

4.2 Crust and the crust−mantle boundary

From south to north over a stretch of more than 900 km the stations of the TOR and neighboring GRSN networks (Fig. 4.1) provide a seismic profile from Paleozoic to Precambrian northern Europe as shown in Fig. 4.2. This section could be considered as a chronological cross section which is similar to the one presented by *Gossler et al. (1999)*, also in receiver function analysis. I have used here the additional data from seven GRSN stations which are in the vicinity of TOR network to improve on the previous results.

The upper section (Fig. 4.2a) has been produced by first move−out correcting the receiver functions and then stacking them from south to north in a procedure called 'moving average'. The idea is to stack the receiver functions in a window (here 50 km wide) which moves in intervals (here 10 km) until the entire extent of the network is swept. By taking this approach the desired P−to−S signals are amplified whereas the background noise and the crustal multiples are considerably weakened.

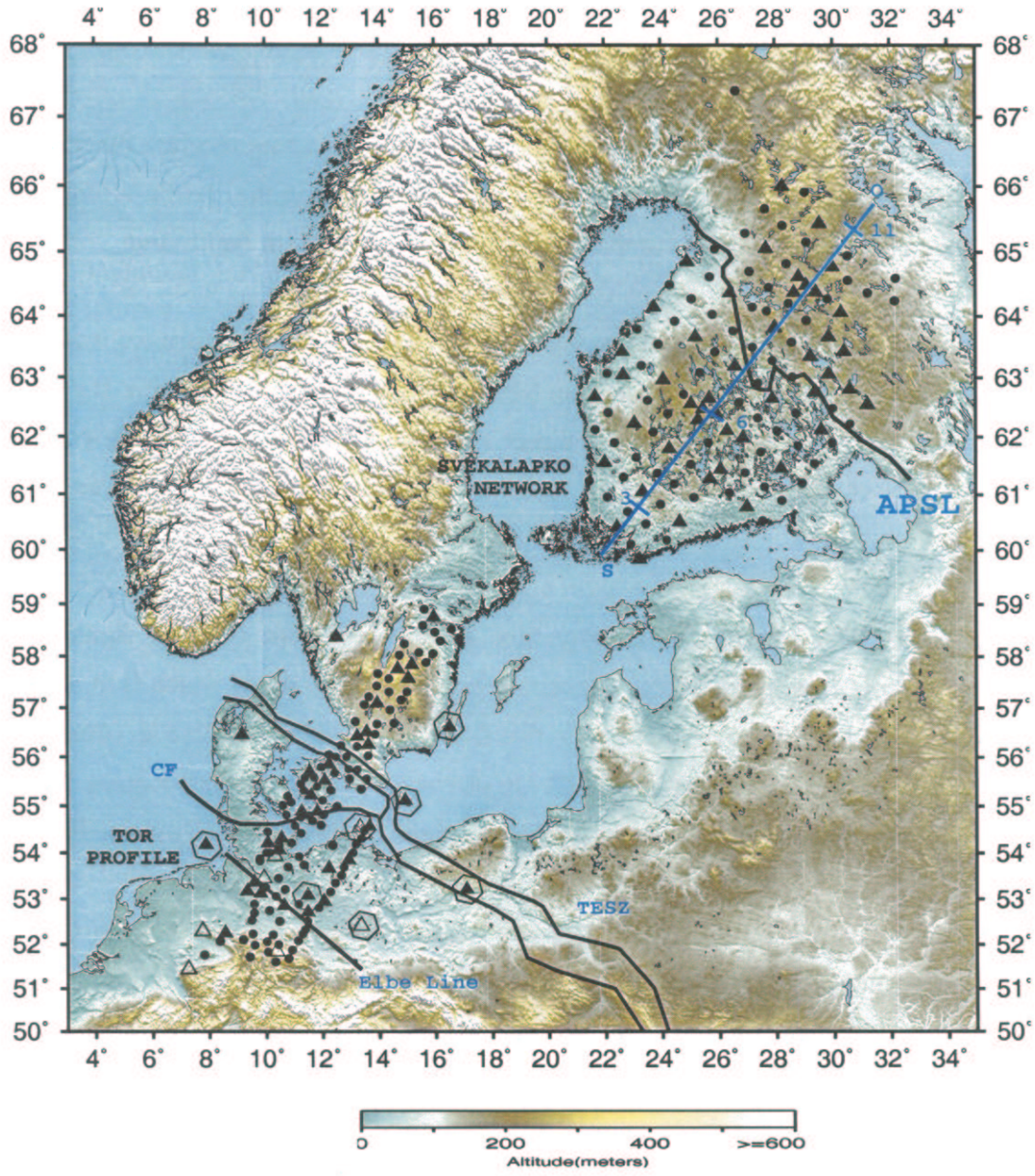

Fig. 4.1 Location map showing the seismographic stations of TOR, SVEKALAPKO, GRSN, and GEOFON networks. The Elbe Line, the Caledonian Front (CF), the Trans−European Suture Zone (TESZ) and the Line of suture between Proterozoic and Archean provinces (APSL) have been depicted and annotated accordingly. Broadband and short period stations have been delineated with triangles and circles, respectively, while the hollow triangles represent the stations of GRSN. The triangles delimited by polygons represent GEOFON stations.

The lower section (Fig. 4.2b) is the result of first migrating the same receiver functions (used for producing Fig. 4.2a) into the space domain and then stacking the result along a south−north section. This enables direct comparison of the delay time with depth data.

The southern part of both sections in Fig. 4.2 is dominated by Paleozoic and younger sedimentary layers filling the North German Basin. Strong Ps conversions from the bottom of the basin arrive up to 1.5 sec after the direct P arrival in time domain (Fig. 4.2a) which correspond to a sedimentary cover of over 10 km observed in the migrated section (Fig. 4.2b).

The conversions from crust−mantle boundary across the North German Basin are bent downwards and observed with delays between 4 and 5 sec (Fig. 4.2a) which is in accordance with receiver function observations along the DEKORP−BASIN '96 profile (*Gossler et al. 1999*). The corresponding depths of 35−40 km observed in the migrated section (Fig. 4.2b) are also in agreement with deep seismic sounding results (*Hoffmann et al. 1996*).

The northern boundary of the North German Basin is considered to be the Caledonian Deformation Front (CDF) (Fig. 4.3) which extends according to seismic interpretations (e.g., *Thybo 1990*, *BABEL Working Group 1993, MONA LISA Working Group 1997a* and *b*) from Poland to the North Sea. However, the transition from the crust of the German Lowlands to that of the Baltic Shield, according to Fig. 4.2, takes place gradually in a complex zone between the Elbe Line and the Tornquist Zone. While the Central European Moho (Avalonia) continues at the depth of about 40 km northwards past the Elbe Line, a second branch−Scandinavian Moho (Baltica), appears at the depth of 30−35 km south of the CDF. This branching of the Moho can be interpreted as subducting Central European Moho under the Scandinavian Crust, a possible remnant of the collisional tectonics dating from the Paleozoic time. The overlying Precambrian crust of the Baltic Shield, north of the CDF can explain why the age determination of some bore−hole samples of the basement north of the CDF (*Larsen 1971)* are in the range of 800 −900 Ma which suggest their Precambrian Baltic Shield origin. Fig. 4.2 fails though to furnish convincing evidence for south dipping intracrustal structures

as *BABEL Working Group (1993)* and recently *DEKORP−BASIN Research Group (1999)* and *Thybo (2000)* associate with the CDF and *Gossler et al. (1999)* referred to as "crocodile structure" following the terminology coined by *Meissner et al. (1991)*.

North of the CDF there is a drastic decrease of the sediments thickness accompanied by a rise of the Moho (from about 35−40 km to 30 km, Fig. 4.2) which is attributed to the inversion tectonics in Cretaceous−Tertiary (*EUGENO−S Working Group 1988*) and characterizes the northwest extension of the TESZ , known as the Tornquist Zone. The elevated Moho was observed by *Kind et al. (1997)* as an offset in delay times of Moho conversions in a receiver function study carried out on data from a temporary deployment of stations (TOR pilot project) across the Tornquist Fan in Denmark and Sweden.

There is a pronounced thickening of the crust observed north of the TESZ towards the Baltic Shield which is which is well known from active seismic (e.g. EUGENO−S Working Group 1988) and receiver function (*Gossler et al. 1999*) studies. Despite the increasing crustal thickness there is up to 50 mGal increase in Bouger gravity anomaly (*EUGENO−S Working Group 1988)* (Fig. 4.4). This discrepancy could be explained by the existence of dense materials in the lower and upper crust which are the sources of contrast and P−to−S conversions observed both in time and space sections (Fig. 4.2). The high velocity material of the lower crust has been explained by underplating −solidification of magma in lower crust during Permian−Carboniferous magmatism (*Thybo et al. 1994*) or alternatively as remnants of subduction or underthrusting of Avalonia underneath the Baltica proposed by *BABEL Working Group (1993)*. The latter hypothesis finds support by this observation as indications of subducting Central European Moho beneath the Scandinavian crust are seen in Fig. 4.2 and as explained above.

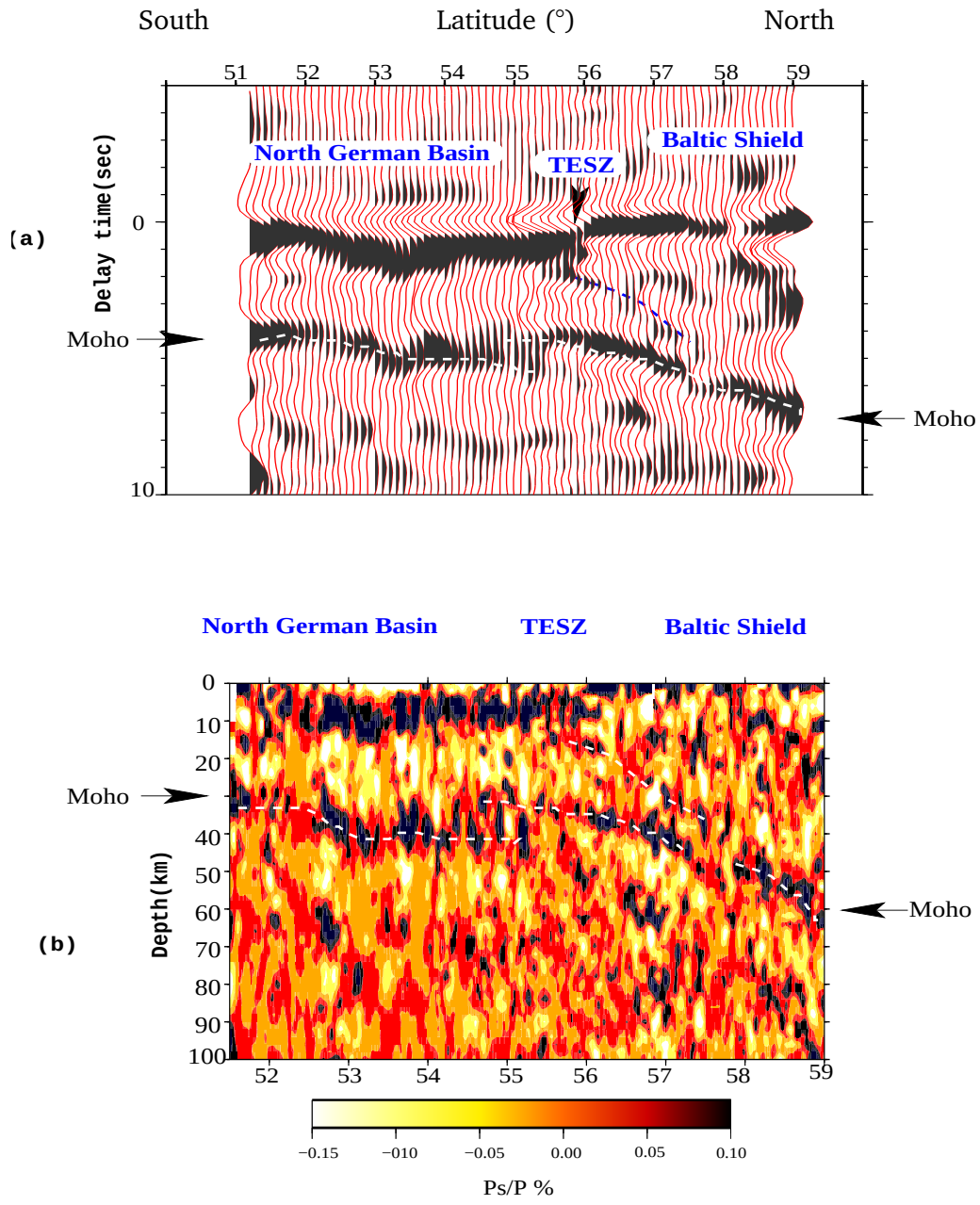

Fig. 4.2 (a) A time domain south−north section of move out corrected receiver functions along the TOR profile, stacked in 50 km wide windows with moving intervals of 10 km and hence providing 80% overlapping between adjacent windows. (b) A migrated and interpolated south−north section of receiver functions along the TOR profile. In both sections the dark positive amplitudes represent the increase of the S−wave velocities with depth. To eliminate low frequency noise a high pass filter with he corner frequency of 0.2 Hz has been applied to the data.

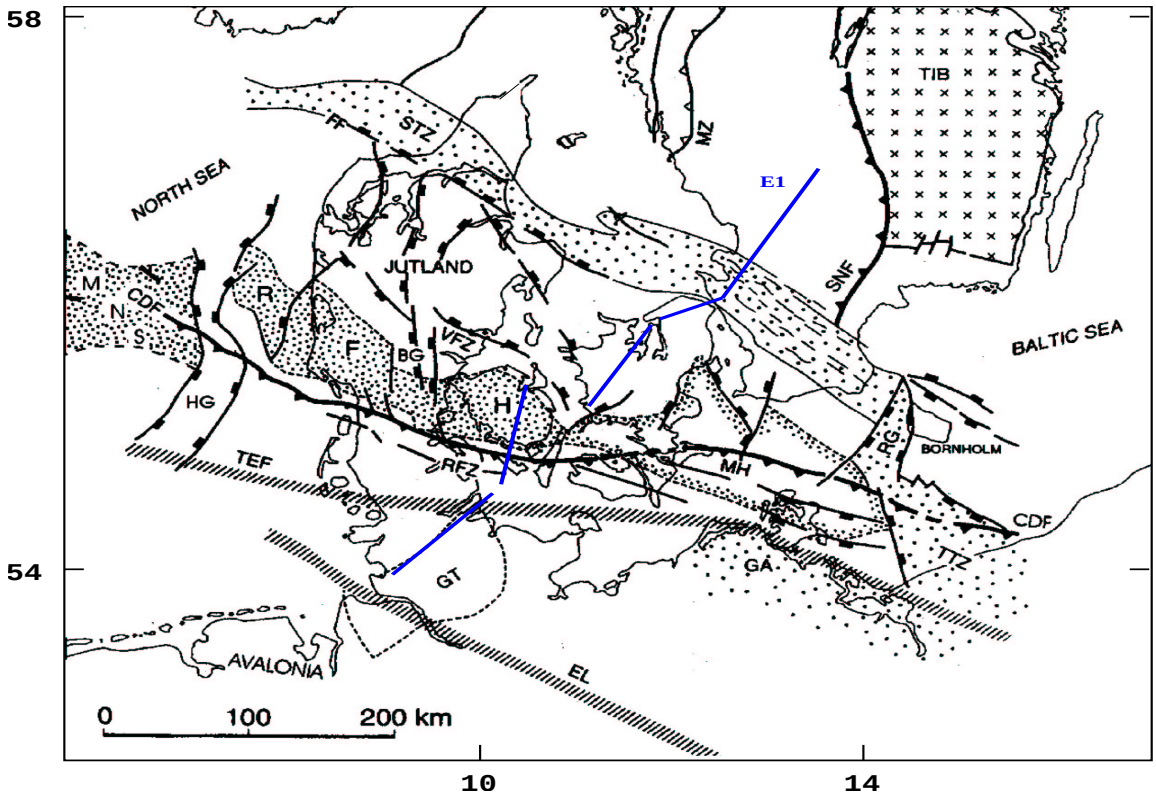

Fig. 4.3 A map showing major structural units in Northern Germany, Denmark and Scandinavia as discussed in the text. The location of the E1 seismic profile (*EUGENO−S Working Group 1988*) is depicted and labeled.

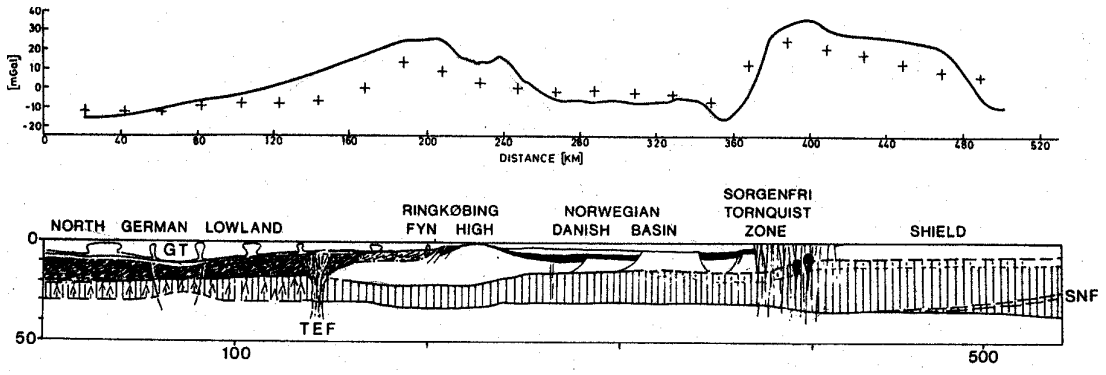

Fig. 4.4 Section along the E1 profile (from *EUGENO−S Working Group 1988)* (Fig. 4.3) showing the Bouger anomaly on top of a simplified sketch of the crustal structure along the profile. Positive Bouger anomaly north of the Tornquist Zone despite deepening Moho can be explained by intracrustal dense materials (refer to the text).

With a gap of around hundred kilometers northeast of the TOR network the stations of the SVEKALAPKO network spread over southern and central Finland (Fig. 4.1). Unlike the German Lowlands there are no significant sedimentary layers over the bedrocks. This reduces scattering of the signals and provide better resolution. Capitalizing on this advantage the threshold of the teleseismic earthquakes was reduced to 5.7 compared to 5.9 for TOR data (sections 2.2 and 2.3).

Fig. 4.5 which has been produced with the same parameters and using the same techniques as Fig. 4.2 is a receiver function cross section from south to north centered around the 27° longitude. As it is obvious in both time domain (Fig. 4.5a) and migrated (Fig. 4.5b) sections there is almost no sedimentary cover over the bedrock. The section starts in Proterozoic domain in the south and by crossing the Archean−Proterozoic Suture Line reaches the Archean nucleus of the Baltic Shield in the north. The crust−mantle boundary is clearly seen in time and space domains (Figs. 4.5a and 4.5b, respectively). Between 61.5°N and 62°N the Moho plunges from about 40 km to beyond 60 km depth (Fig. 4.5b). Further to the north, at about 65.5 °N it rises smoothly to the depth of 40−45 km . The sudden deepening of the Moho occurs about 100 km south of the surface trace of the suture zone (Fig. 4.1 & Fig. 4.6) between the Proterozoic and Archean parts of the Baltic Shield. The offset of the Moho is accompanied by some north dipping structures observed in sections which we attribute to the subduction and collision of the Proterozoic and Archean orogenies. Such interpretation is in agreement with the results of "Babel 4" seismic reflection experiment (*BABEL Working Group 1990*) which was carried out in a nearby region across the Gulf of Bothnia (Fig. 4.6 & Fig. 4.7).

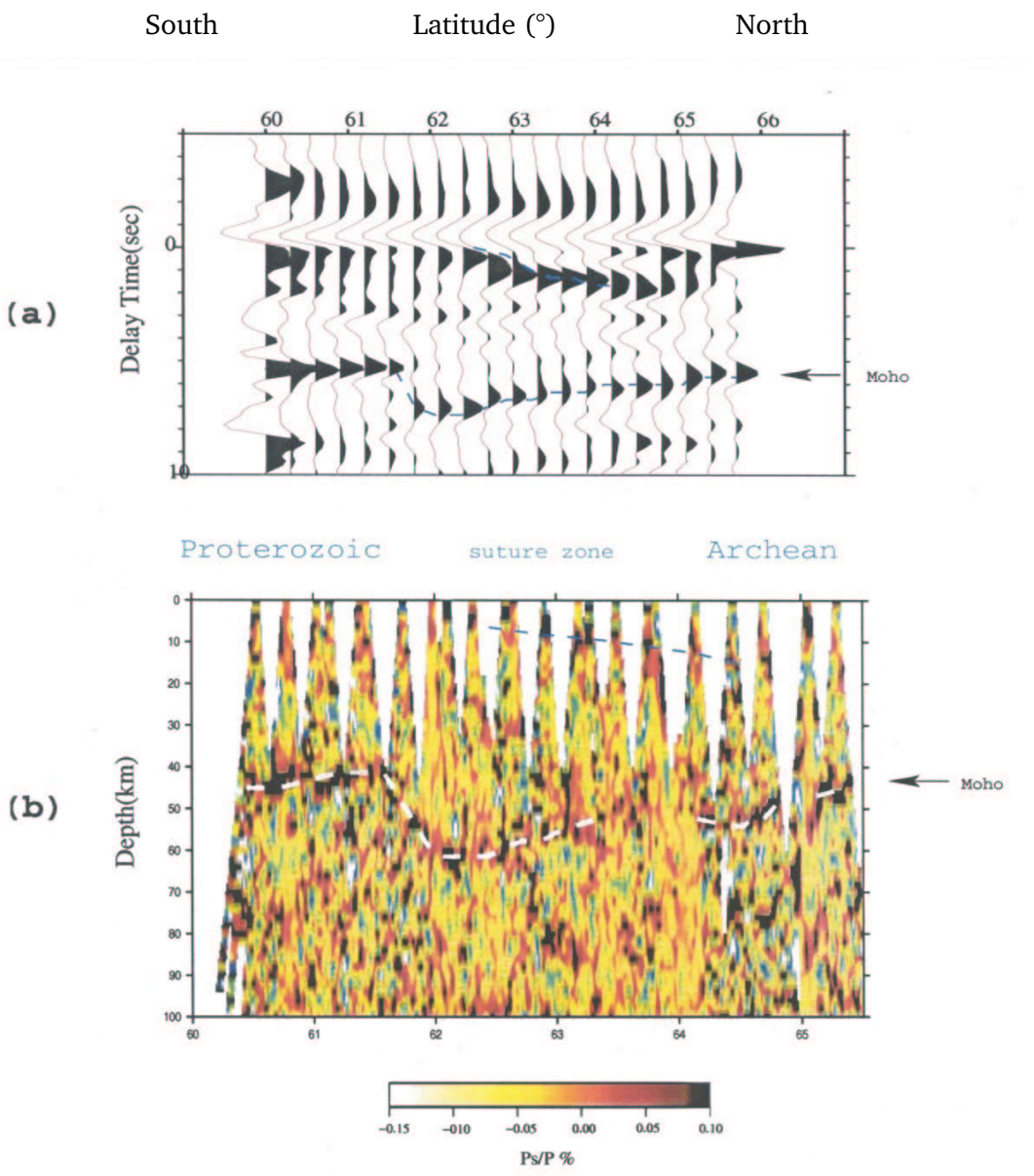

Fig. 4.5 South−north oriented sections of the receiver functions in Time (a) and space (b) domains, in a 2° wide strip centered around 27°E across the SVEKALAPKO network. Receiver functions were high passed by a filter with the corner frequency of 0.2 Hz to eliminate the low frequency noise. Receiver functions in time domain (a) have been stacked from south to north in 50 km wide windows with moving intervals of 10 km. In both sections we observe a sudden deepening of the Moho by more than 20 km just south of the line of suture between Proterozoic and Archean orogenies. The offset of the Moho is accompanied by lack of negative Bouger anomalies (*Elo 1999)* and north dipping intracrustal structures.

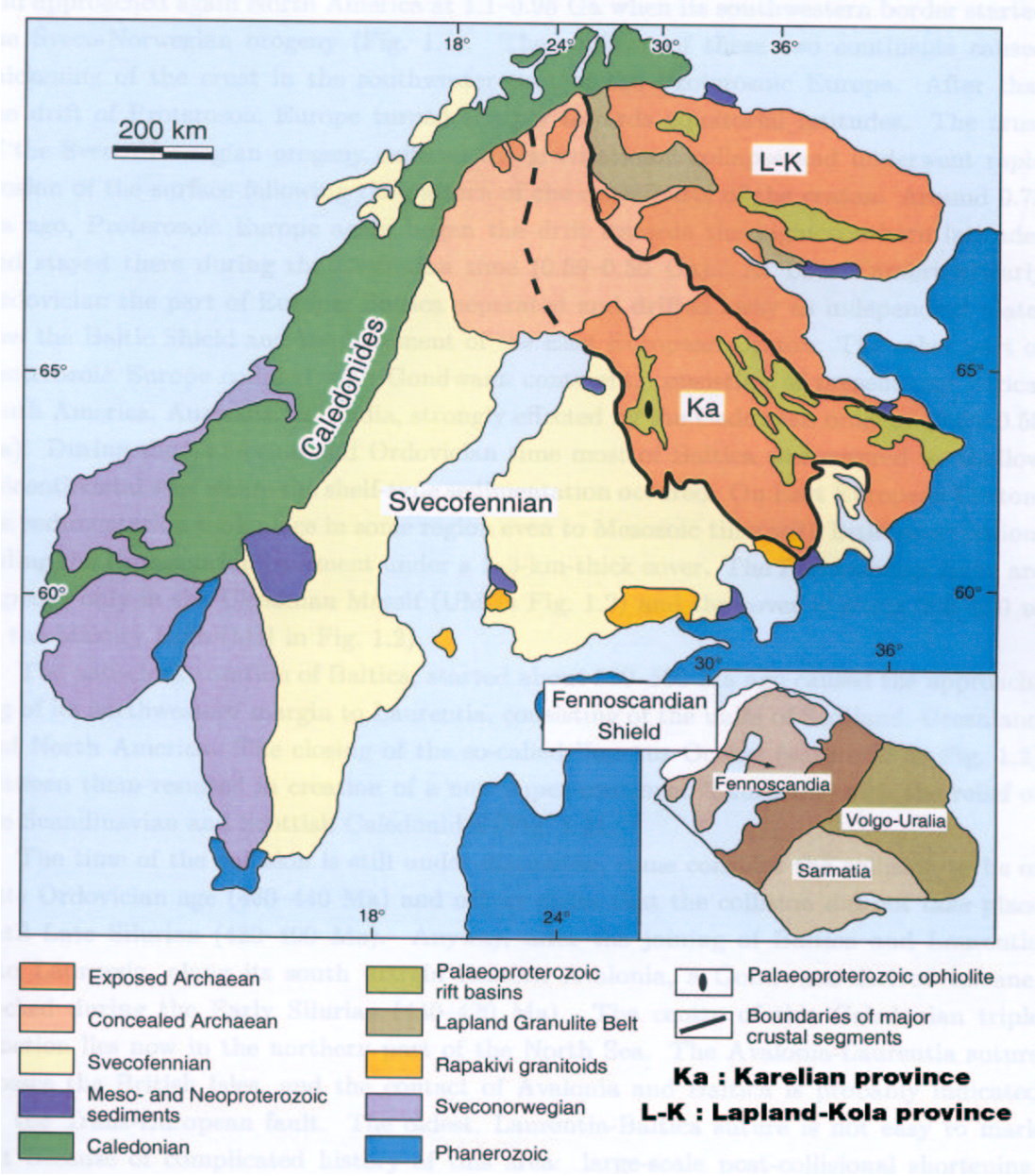

Fig. 4.6 simplified map showing the main structural units in the Baltic Shield (after *Hjelt & Daly 1996*). The **APSL** represents the Archean−Proterozoic Suture Line). The location of the BABEL 4 profile (*BABEL Working Group 1990*) in the Golf of Bothnia is labeled as **B**. The small map in the corner delineates subdivisions within the East European craton.

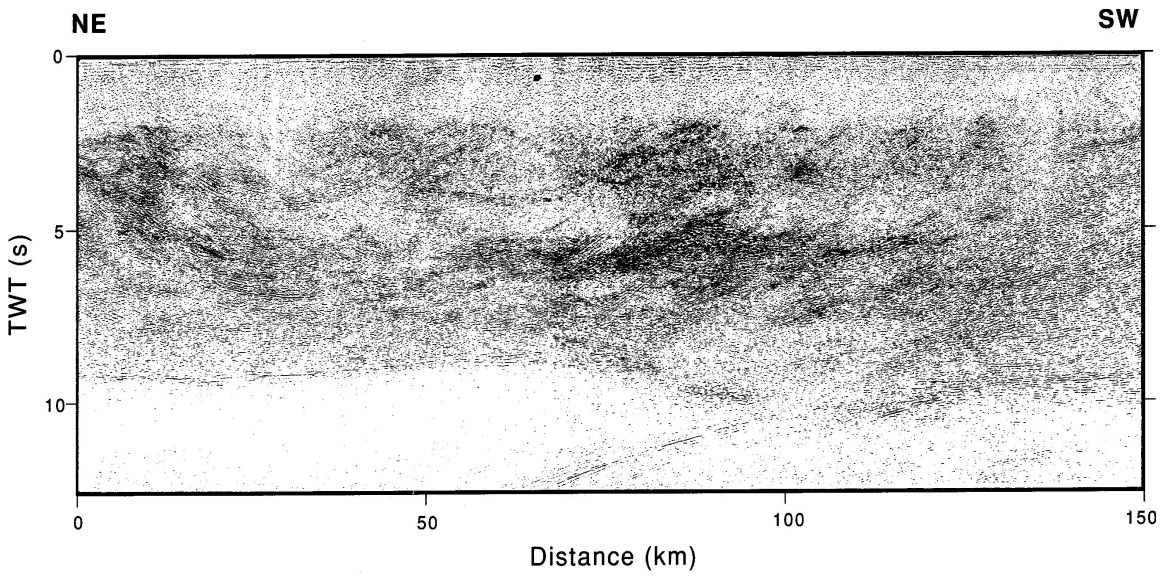

Fig. 4.7 Seismic cross section along the Babel 4 profile (*BABEL Working Group 1990*) in the Golf of Bothnia (Fig. 4.6) showing reflectors dipping northeast and southwest, as evidence for the subduction and collisional tectonics associated with the suture line between Proterozoic and Archean provinces in the Baltic Shield.

The observation of phenomenal Moho topography along the presented sections of TOR and SVEKALPKO (Fig. 4.2 & Fig. 4.5) demanded mapping of Moho delay times as well as the crustal thickness across the two networks. Unlike the stations of the SVEKALAPKO network which provided rather good quality receiver functions for measuring delay times it was necessary to apply a special space stacking method to the TOR data. The method consisted of first calculating the conversion points of all receiver functions at an assumed depth of the Moho (here taken as 35 km). Stacking of all receiver functions was then performed in cells of 50 km $\times$ 50 km dimensions which moved in 30 km intervals along latitude and longitude directions to sweep the entire range of the network. Next, Moho delaytimes for each cell where possible were read and assigned to the center of the cell (Fig. 4.8).

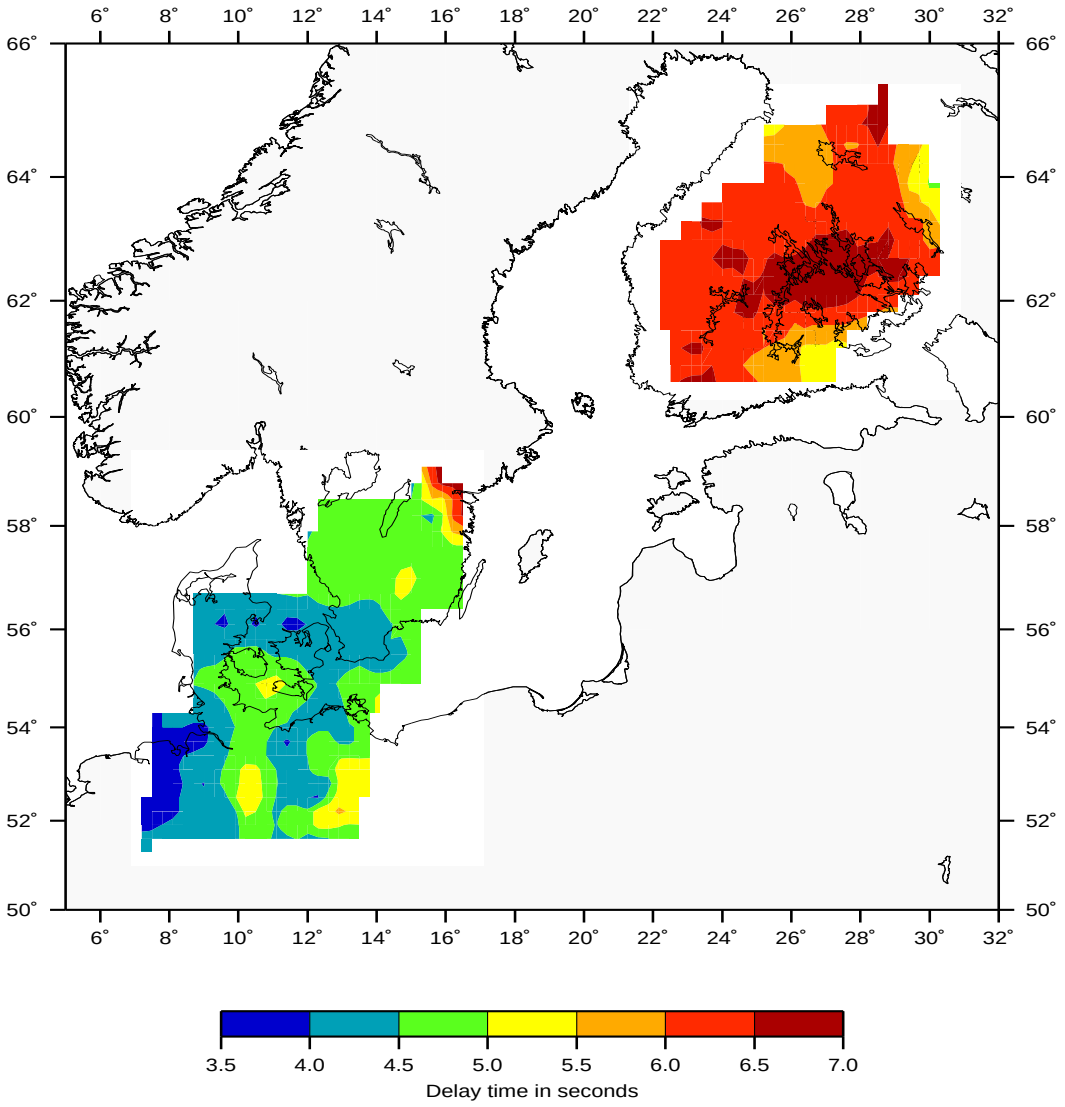

Fig. 4.8 Map of the delay times of the Moho conversion phases across the TOR and SVEKALAPKO networks measured relative to the direct P arrival. A decrease in delay time across the Tornquist Zone is clearly observed which can be explained by the elevated Moho in response to inversion tectonics involved. Northeast of the TESZ towards the Baltic Shield a steady increase in the delaytime as a result of increasing Moho depth is obvious. Across the SVEKALAPKO there is a significant maximum in the delaytimes which is located in the immediate south of the Archean−Proterozoic Suture Line.

The result of visual examination and reading of delay times for all cells across the TOR network and for individual stations over the SVEKALAPKO is presented in Fig. 4.8. It shows clear increase of Moho delay times north of the Tornquist Zone and a significant delay of the Moho conversion south of the Archean−Proterozoic Suture Line.

To translate the measured Moho delay times into crustal thickness a prior knowledge of average Vp/Vs ratio of the crust is needed. *Zhu & Kanamori (2000)* have intoduced as discussed in section 3.5 a method for estimating crustal thickness which does not make use of the delay time data. Nor is it necessary to have information on the Vp/Vs . In fact both crustal thickness and Vp/Vs values are the output of the method (Fig. 4.9). Using this technique a map of the crustal thickness was produced (Fig. 4.10) which shows an expected resemblance to the map of Moho delay times (Fig. 4.8).

In Fig. 4.10 the resulting depths to the Moho is color coded whereas the white color contours represent the Moho depths compiled from controlled seismic source investigations (*EUGENO−S Working Group 1988, Luosto 1997, Korsman et al. 1999*). At the southern end of the TOR profile the Moho depth is about 30 km and reaches near 40 km in a strip below and parallel to the Elbe Line. Below the Danish Basin the Moho is again shallowing to about 30 km. It is worth mentioning that the continuation of the Central European Moho (the branch under the North German Basin) at about 40 km depth from north of the Elbe Line to the Tornquist Fan (Fig. 4.3) is not seen in the map view of Fig. 4.10. North of the 56 °N parallel and into the Baltic Shield the crustal thickness increases rapidly.

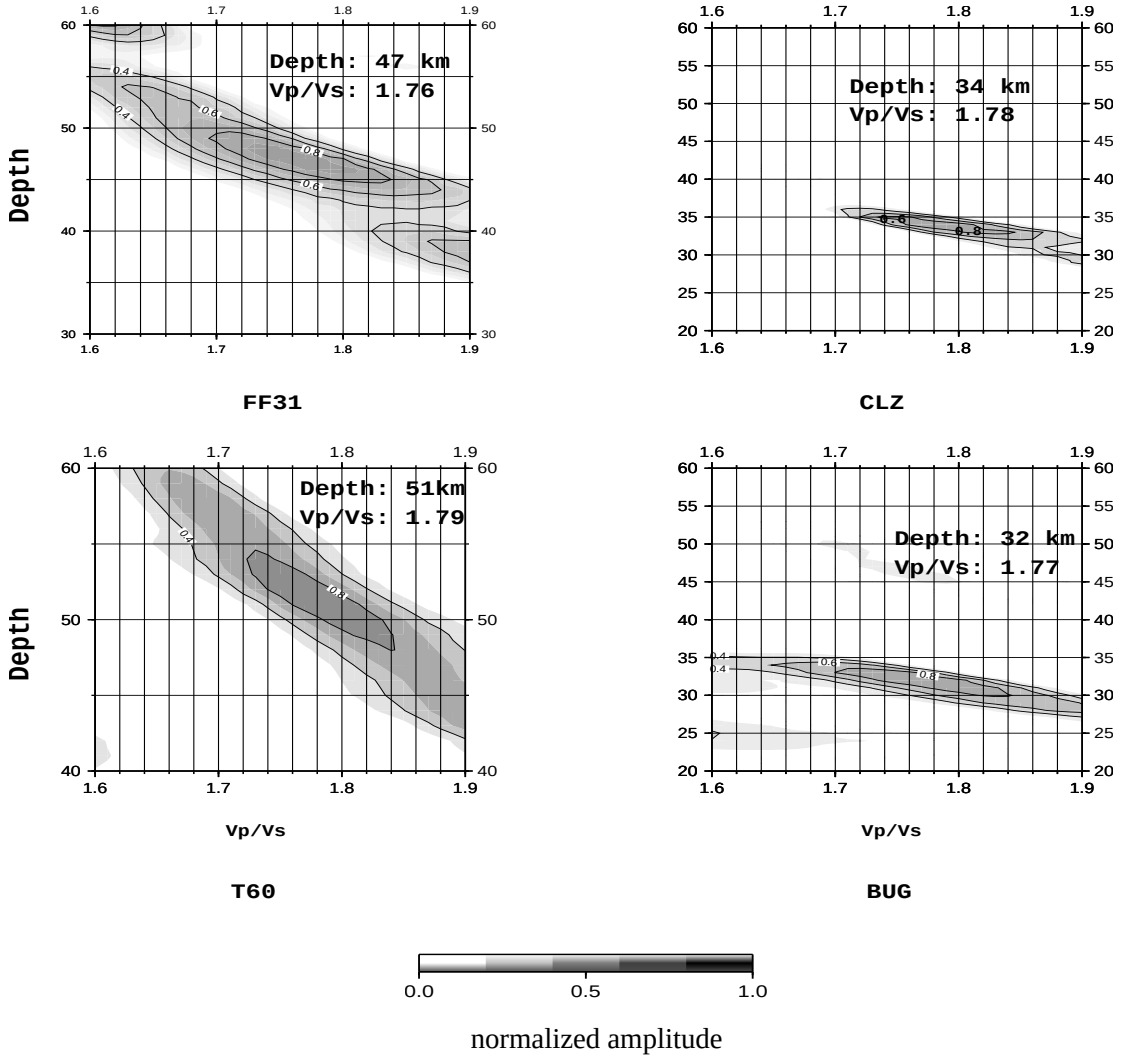

Fig. 4.9 Examples of successful application of the *Zhu & Kanamori (2000)* method to receiver functions from 2 permanent stations of the GRSN, i.e., **BUG** and **CLZ** (Table B.3, Appendix B) and two temporary stations in TOR and SVEKALAPKO networks, i.e., **T60S** (Table B.1, Appendix B) and **FF31** (Table B.6, Appendix B), respectively. The best values of the crustal thickness vs. Vp/Vs are highlighted in each panel.

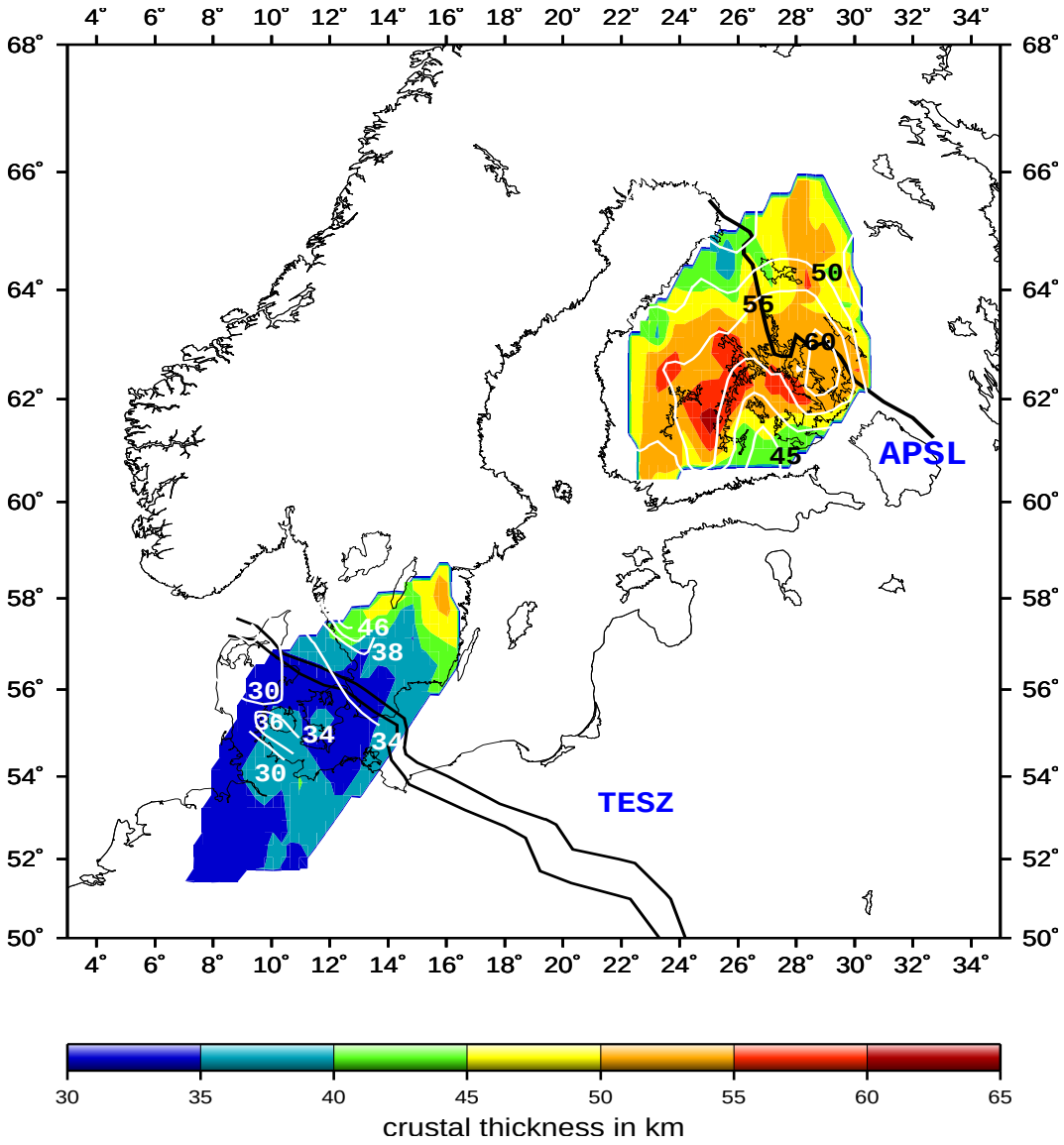

Fig. 4.10 A color coded map of the crustal thickness across the TOR and SVEKALAPKO networks as calculated by applying Zhu & Kanamori method (*Zhu & Kanamori 2002*) to the receiver function (RF) data. Superimposed are the white color contours which represent the data from the controlled seismic source (CSS) studies (*EUGENO−S Working Group 1988, Luosto 1997, and Korsman et al. 1999)*. There is a great deal of agreement between the results of the two data sets. A discrepancy shows up in central Finland where the deepest Moho offset according to the RF results is located southwest of the suture line of the Proterozoic and Archean provinces (APSL), which is in contrast with the CSS inferred results.

Underneath the SVEKALAPKO network, the Moho takes a complex topography with the deepest point south of the Proterozoic−Archean suture line. The abrupt variations of the crustal thickness is in contrast to the quite flat surface topography and lack of negative Bouger anomaly (*Elo 1999*). One explanation for this apparent contradiction is the assumption of high density middle or lower crust which might be the result of magmatic intrusions and underplating that are associated with the collision of plates and the process of crustal thickening (*Korsman et al. 1999*).

Fig. 4.11 shows the distribution of the Vp/Vs values across TOR and SVEKALAPKO networks as obtained by application of Zhu & Kanamori method (*Zhu & Kanamori 2000*) to receiver function data from recording stations. Although the values, due to insufficient quantity of data needed for a thorough investigation of this kind, demand cautious treatment, one can identify a noticeable increase of Vp/Vs values across TESZ. This is in agreement with the recent findings of *Wilde−Piorko et al. (2002)*.
Across the SVEKALAPKO network the values do not show significant variations and are well within the range expected from stable cratons.

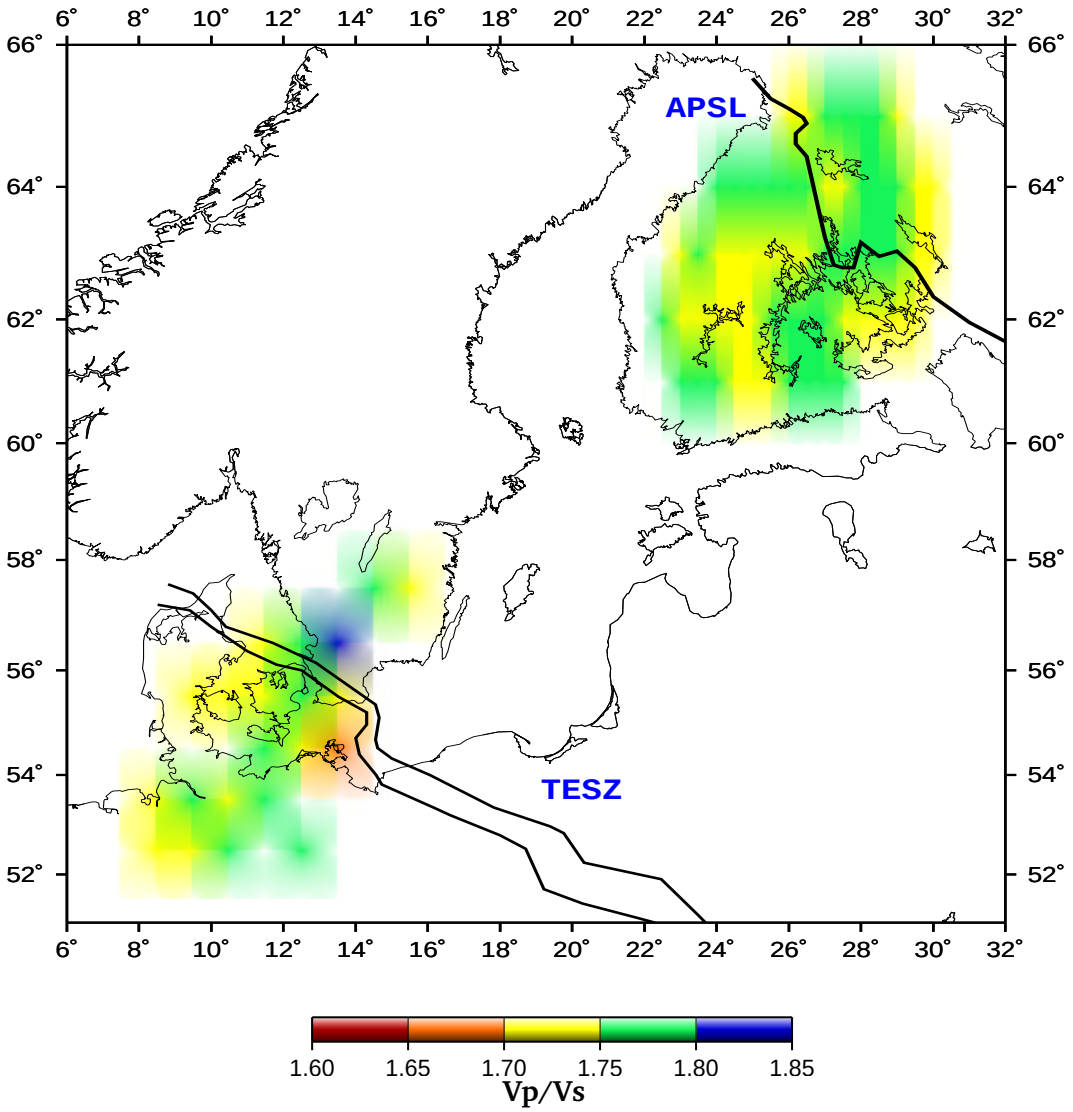

Fig. 4.11 Distribution of Vp/Vs values across the TOR and SVEKALAPKO networks as determined by applying the Zhu & Kanamori method (*Zhu and Kanamori 2002*) to the receiver function data. An increase towards higher values of Vp/Vs values is observed north of the TESZ whereas across the SVEKALAPKO network the values do not show abrupt variations and are within the range expected from stable cratons.

4.3 Upper mantle discontinuities

Receiver function methodology is a powerful tool for probing the upper mantle in search for major upper mantle discontinuities and unraveling the characteristics of transition zone between the 410 km and 660 km discontinuities. Both discontinuities are globally observed and are believed to be associated with phase transitions rather than bulk changes in composition (*Lay and Wallace 1995*). The abrupt change in seismic impedance responsible for producing Ps conversions is therefore due to transition to denser lattice structures with increasing pressure and temperature (*Press and Siever 1978*). Although the depth of the discontinuities is assumed to be constant on a global scale, topographical changes due to thermal variations have been reported (e.g. *Lay 1992, Shearer 1993, Gossler & Kind 1996*).

Because of the attenuation and scattering of already weak converted phases that originate from the upper mantle discontinuities and travel through the heterogeneous upper mantle and crust, it is necessary to stack receiver functions. Whereas move out correction prior to stacking is marginally important for amplification of Moho conversion signals (section 3.3) it is extremely crucial for identifying upper mantle discontinuities. Stacking the distance equalized receiver functions amplifies the amplitude of the converted phases by constructive summation while weakens the background noise which is assumed to be white noise and of random nature. A combination of moving average stacking technique and low pass filtering of the receiver function has been used. By moving average stacking of distance equalized receiver functions in terms of the latitude of their P−to−S conversion points at the depth of 520 km (Fig. 4.12), it became possible to detect and identify the 410 and 660 km discontinuities beneath the TOR and SVEKALAPKO networks.

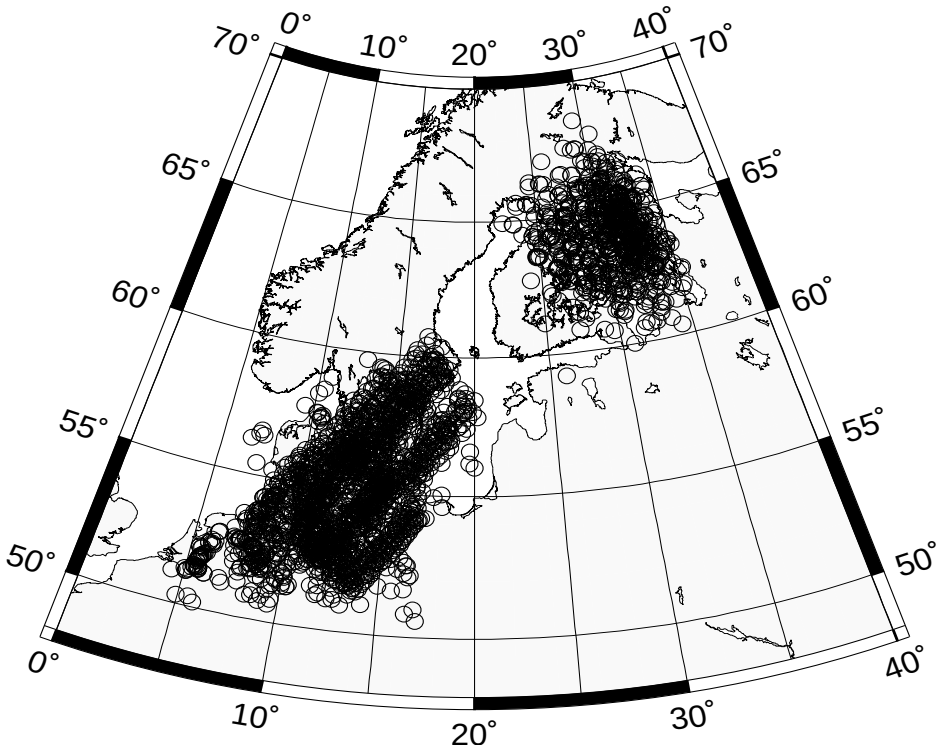

Fig 4.12 Map of distribution of conversion points at the depth of 520 km (hollow circles) for receiver functions recorded at TOR and SVEKALAPKO networks, calculated using IASP91 global velocity model (*Kennett & Engdahl 1991*). Their coordinates have been taken as average for conversion points at depths of 410 km and 660 km and used for spacial stacking .

Fig. 4.13 shows south−north oriented cross sections of stacked receiver functions along TOR (lower section) and SVEKALAPKO (upper section) networks. Both discontinuities are visible in the data of both networks. The location of the 410 discontinuity is over the entire TOR profile (52−59°N) in fairly good agreement with the IASP91global velocity model. This agreement continues to the southern end of the SVEKALAPKO profile (up to about 61°N). North of that latitude the 410 arrives up to 2 sec earlier than predicted by IASP91. This is apparent in the summation traces at the top of the Fig. 4.13.

The 660 discontinuity appears at the southern end of TOR up to 3 sec earlier than IASP91. This signal is however relatively weak and it could be influenced by multiples of other upper mantle phases. It seems unlikely that only the 660 and not the 410 is affected by relatively hot transition zone. At the northern end of TOR the 660 appears at normal times. Across the SVEKALAPKO the 660 conversion appears earlier, especially at the northern end, in agreement with the earlier 410. The summation traces of all TOR and SVEKALAPKO data (top of the Fig. 4.13) show clearly that the differential times of the 410 and 660 are in good agreement with IASP91. Both discontinuities are however $1-2$ sec earlier, especially at the northern end of SVEKALAPKO. This is very likely due to an about 5% faster upper mantle at the Archean Baltic shield, an indication of higher shear velocity in upper mantle of the Baltic shield, a result well in agreement with latest teleseismic body wave (*Sandoval et al.* 2001) and surface wave (*Funke & Friedrich 2001*) tomography studies and consistent with what is expected from stable shields (SNA velocity models, *Grand & Helmberger 1984*).

Fig. 4.14 is produced by first stacking the move−out corrected receiver functions according to the geographical coordinates of their conversion points at the depth of 520 km in cells of 100 km $\times$ 100 km dimensions spread over the entire extent of TOR and SVEKALAPKO networks and then mapping the measured the delay times of 410 with respect to IASP91 arrival time of the 410 phase. It could be envisaged as an indication for earlier arrival of 410 conversions north of the Tornquist Zone and across the entire expanse of the SVEKALAPKO network.

By examining the migrated receiver function image of the SVEKALAPKO (Fig. 4.15) it is observed this time in space domain that 410 km and 660 km conversion phases arrive markedly earlier than predicted by IASP91 velocity model, quite consistent with the time domain section (Fig. 4.13). Besides, clear 660 signal compared to rather fuzzy 410 appearance could be attributed to inherent sharpness of 660 and to heterogeneities at depths down to 410 discontinuity.

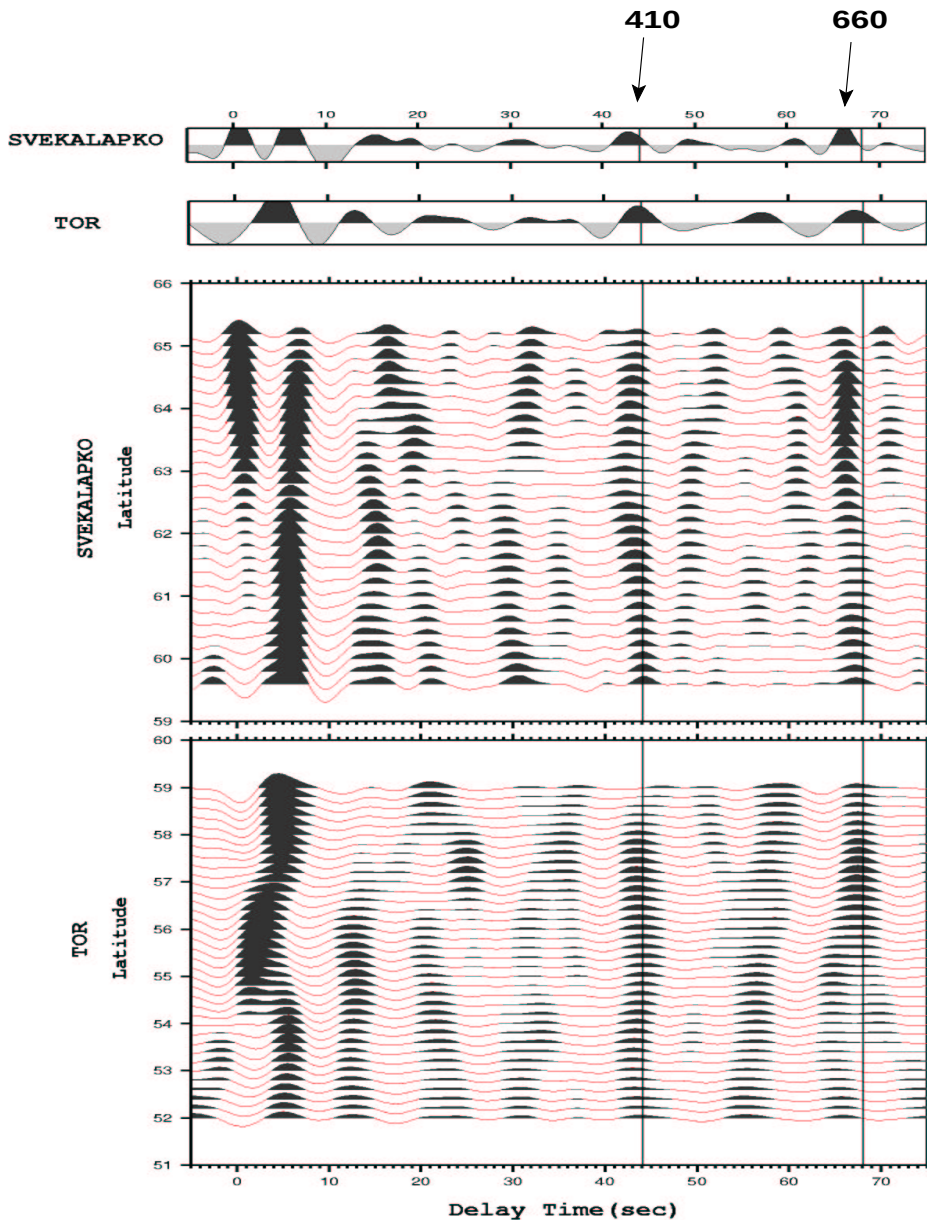

Fig. 4.13 South−north sections of the receiver functions along the TOR (lower part) and SVEKALAPKO (upper part) networks, stacked by latitudes of Ps conversion points at the depth of 520 km in windows of 100 km wide with moving intervals of 30 km. Traces have been low pass filtered (corner frequency of 0.2 Hz). This and the fact that traces are stacked according to their conversion points at the depth of 520 km makes these sections unsuitable for tracing the Moho with high resolution while it proves to be an efficient tool for enhancing the converted phases from the 410 km and 660 km discontinuities. Vertical lines indicate the expected IASP91 (*Kennett & Engdahl 1991)* arrival times of Ps conversions from 410 km (at 44.08 sec) and 660 km (at 68.06 sec). Across the SVEKALAPKO km and 660 km conversions arrive 1−2 sec earlier than predicted by IASP91 global velocity model.

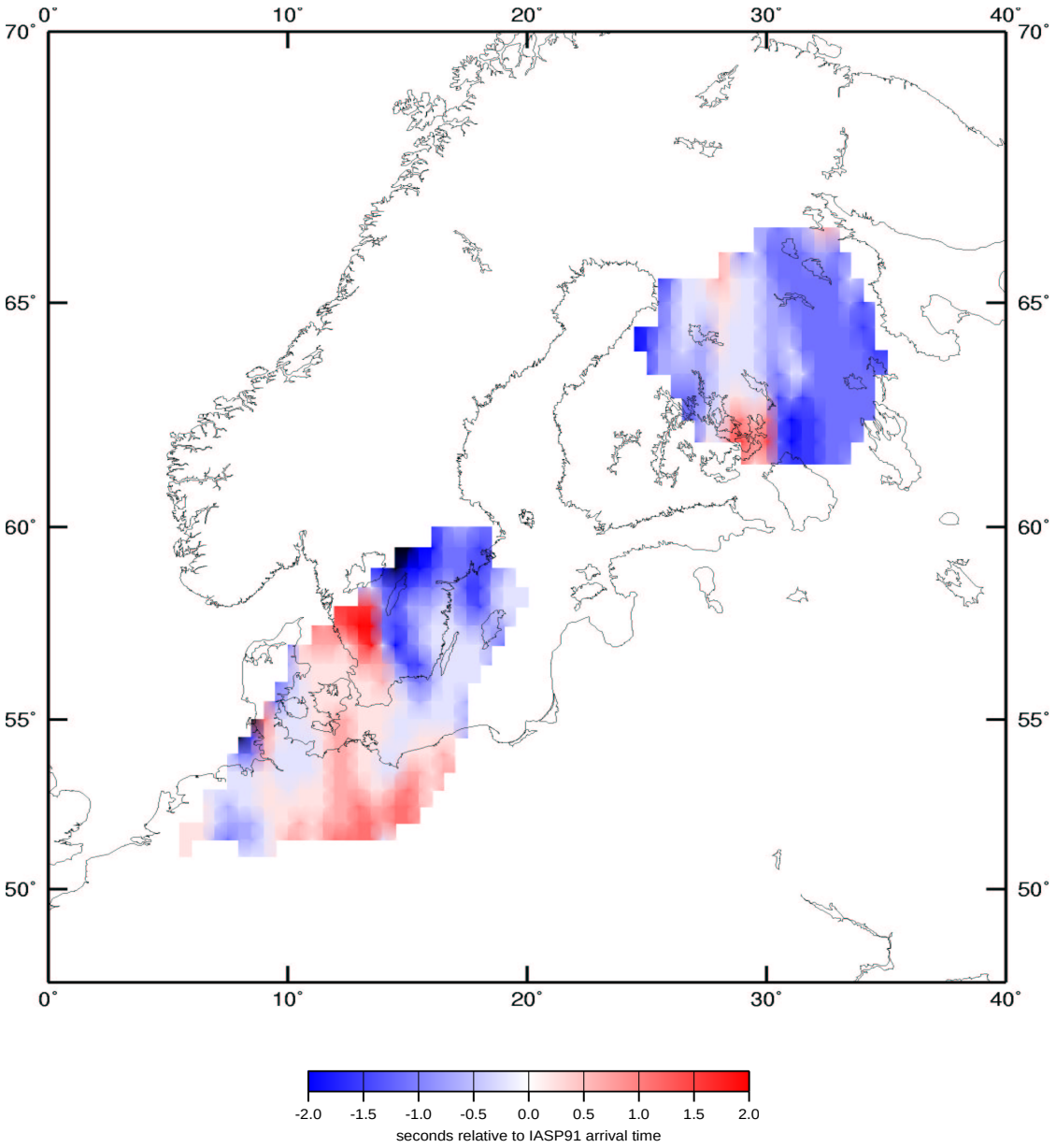

Fig. 4.14 Map showing the differences between observed and IASP91 predicted arrival times of 410 km conversions across TOR and SVEKALAPKO networks . Zero on the bar scale marks the theoretical arrival time of 44.08 sec of 410 km conversion phase with respect to the direct P onset. North of the Tornquist Zone and all across the SVEKALAPKO network the arrival times of the 410 km conversion phase is ahead of the time predicted by IASP91 global velocity model.

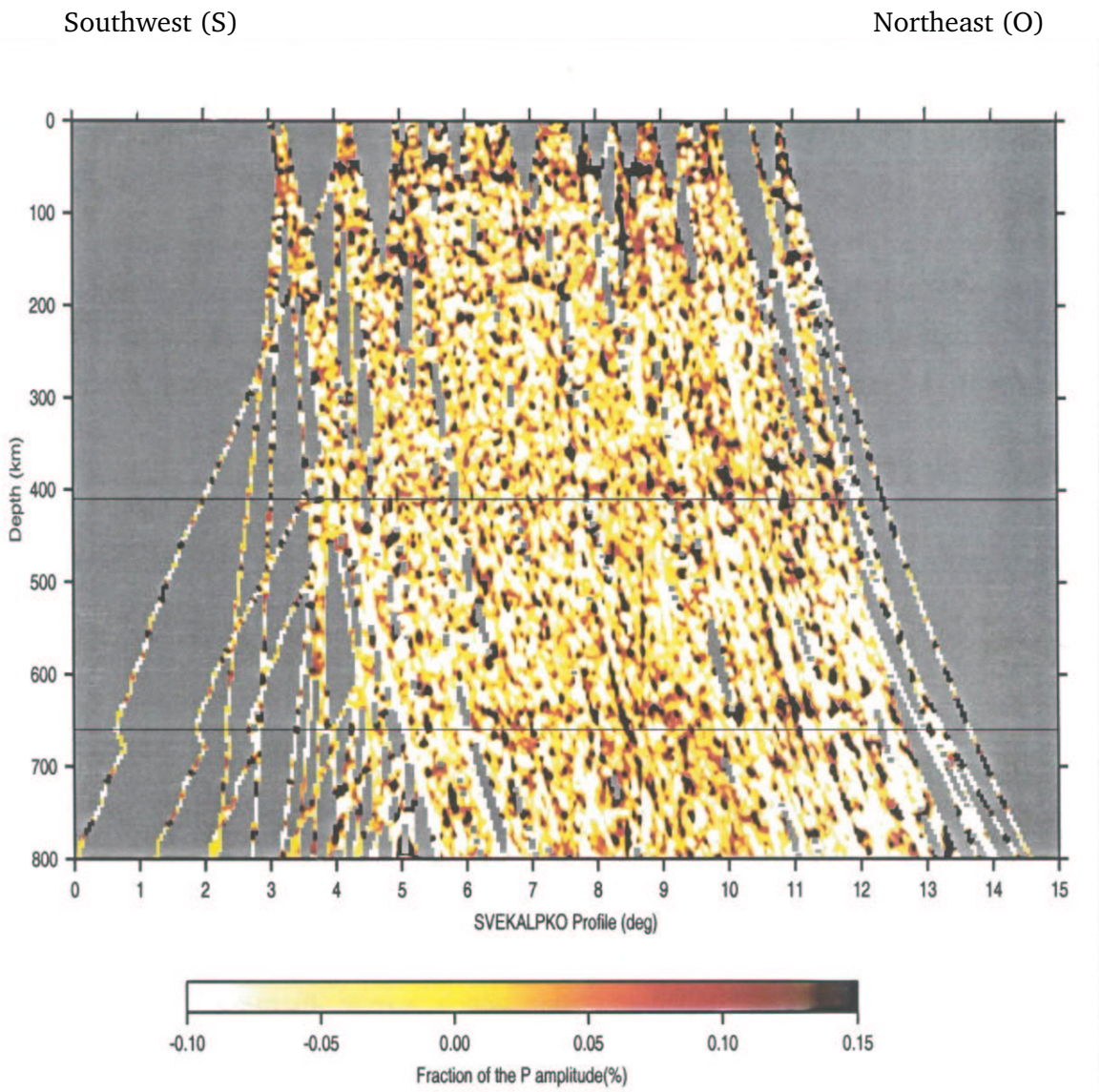

Figure 4.15 Migrated section of the SVEKALAPKO network as projected along SO profile (Fig. 4.1). Both 410 km and 660 km conversions arrive, specially in the Archean province, significantly earlier (1−2 sec, according to Fig. 4.13) than predicted by IASP91 global velocity model